

Increase of the photosensitizing efficiency of the Bacteriochlorin *a* by liposome-incorporation

Xavier Damoiseau^{a,*}, Hans J. Schuitmaker^b, Johan W.M. Lagerberg^b, Maryse Hoebeke^c

^aExperimental Physics, Institute of Physics (B5), University of Liège, 4000 Liège, Belgium

^bBoston Clinics PDT BV, Leiden, The Netherlands

^cCenter of Oxygen Research & Development (CORD), Institute of Physics, B5, University of Liège, Liège, Belgium

Received 17 October 2000; accepted 6 February 2001

Abstract

To describe the action mechanisms of Bacteriochlorin *a* (BCA), a second generation photosensitizer, in phosphate buffer (PB) and in dimyristoyl phosphatidylcholine (DMPC) liposomes we carried out oxygen consumption and ESR measurements. In PB, where BCA was in a monomer–dimer equilibrium, our results suggested that the oxygen consumption was related to the BCA monomers concentration in solution. Incorporation of BCA in DMPC liposomes, by promoting the monomerization of BCA, increased 9-fold the oxygen consumption in comparison to the value in PB. The use of specific singlet oxygen quenchers (Azide and 9, 10-Anthracenedipropionic acid) in ESR and oxygen consumption experiments allowed us to assert that BCA was mainly a type II sensitizer when it was incorporated in DMPC. Finally, the cell survival of WiDr cells after a PDT treatment was measured for cells incubated with BCA in cell culture medium and cells incubated with BCA in DMPC. Irrespective of the dye concentration, the cell survival was lower when liposomes were used. This effect could be the result of a better BCA monomerization and/or a different BCA uptake in cells. © 2001 Elsevier Science B.V. All rights reserved.

Keywords: Bacteriochlorin *a*; Liposomes; Oxygen consumption; Aggregation; Absorption; Fluorescence; Temperature; ESR

1. Introduction

Photodynamic therapy (PDT) is an attractive method for the treatment of certain malignant tumors. The treatment is based on the retention of photosensitizers by cancerous tissues in combination with oxygen and light irradiation. The photosensitizer usually employed in PDT is Photofrin II (PII). PII was applied with favorable results in several thousands of cancer treatments [1]. But, despite its clinical success, PII is not the most optimal sensitizer because of its physical and chemical properties: PII has a low molar absorption coefficient above 600 nm, where the skin penetration of light is optimal, and induces long lasting skin photosensitivity [2].

Bacteriochlorin *a* (BCA), a sensitizer of the second generation [3] has, in methanol, an absorption band centered at 760 nm and a high molar extinction coefficient of 39,000 M⁻¹ cm⁻¹. Oxygen consumption measurements

show that in aqueous solutions BCA is a more effective photosensitizer than HpD [4]. In vivo experiments have shown that BCA has good tumor localizing properties and, upon irradiation, is able to induce the destruction of tumors [3–6].

The efficacy of PDT is determined by several factors: in particular, the localization of the dye in the malignant cells and the ability of the sensitizer to produce reactive oxygen species (ROS) like singlet oxygen (type II reactions) and free radicals (type I reactions) [7–10]. In PB, Beems et al. showed that, upon illumination, BCA was able to induce oxygen consumption. The use of specific quenchers emphasized the presence of singlet oxygen (¹O₂) in the reaction mechanism. Using electron spin resonance (ESR), Hoebeke et al. found evidence that light irradiation of BCA in aqueous solutions led to the production of ¹O₂ and hydroxyl radicals (OH[•]) [11]. Assuming that dimyristoyl phosphatidylcholine liposomes (DMPC) are a simple membrane model, Hoebeke et al. showed that, at 25°C, BCA can be completely incorporated into lipid bilayers in a monomeric form if the lipids to BCA ratio (*R*) is greater

*Corresponding author. Tel.: +32-4-366-3631; fax: +32-4-366-2813.
E-mail address: x.damoiseau@ulg.ac.be (X. Damoiseau).

than 125 [12]. Moreover, in the lipid bilayers, BCA is located only around the polar head region [12]. The influence of BCA incorporation within lipid bilayers on its photodynamic properties (especially the $^1\text{O}_2$ production) is still unknown. Such a study is necessary in order to understand the BCA action mechanism in PDT and eventually to increase the PDT efficiency by using liposomes as drug carriers [13].

The aim of this study is to investigate the photodynamic properties of BCA within liposomes. To achieve this goal, oxygen consumption rate experiments are carried out. The effect of temperature and DMPC concentration are particularly studied. By combining these results with absorption and fluorescence measurements, we show that the increase of oxygen consumption observed when BCA is in DMPC is probably due to the BCA monomerization. The use of quencher in oxygen consumption and ESR spin-trapping experiments emphasizes the presence of $^1\text{O}_2$ in the action mechanism of BCA in liposomes. Finally, WiDr cells were incubated with BCA and irradiated with red light. The influence of the BCA incorporation within DMPC on the WiDr survival is examined by the MTT assay.

2. Materials and methods

2.1. Chemicals

Dimyristoyl-L- α phosphatidylcholine (DMPC) were from Sigma (Belgium). Methanol (MeOH) and chloroform were from J.T.Baker (Deventer, The Netherlands). Histidine and 3-[4,5-dimethylthiazol-2-yl]-2,5-diphenyltetrazolium bromide (MTT) were obtained from Sigma (St Louis, USA). 9,10-Anthracenedipropionic acid (ADPA) was synthesized by Dr Neuray (Iniex) as described by Gandin et al. [14]. 5,5-dimethyl-1-pyrroline-*N*-oxide (DMPO) was purchased from Aldrich Chemical Co. (USA), purified as described previously [15] and stored at -20°C under nitrogen to avoid any oxidation of the spin-trap before the irradiation with the photosensitizer. All others chemicals were of analytical grade and used without further purification.

2.2. Preparation of bacteriochlorin *a*

BCA was prepared as described before [7–9,16]. In short, Bacteriochlorophyll *a* was extracted from the photosynthetic anaerobic bacterium *Rhodospirillum rubrum*. It was purified according to the method of Omata and Murata [17]. Saponifying Bacteriochlorophyll *a*, as described by Oster et al. [18], yielded Bacteriochlorophyllin *a*. In order to remove the Mg central ion, Bacteriochlorophyllin *a* was subjected to acid hydrolysis with sodium acetate (pH 2.0). The BCA formed was extracted with ethyl acetate, which was subsequently evaporated under reduced pressure. The

BCA was then lyophilized overnight and stored at -20°C in the dark and under nitrogen. Purity of BCA was checked by spectrophotometric methods. Throughout the extraction and synthesis procedures, care was taken to work at 4°C and under reduced light intensity.

Before each experiment, a stock solution of BCA in methanol (0.8 mg/ml) was made. Then, the BCA in methanol was added to PB (pH 7) or liposomes solutions at the desired concentration. BCA concentration in methanol was determined by absorption measurement using a value of $39,000\text{ M}^{-1}\text{ cm}^{-1}$ for the extinction coefficient at 760 nm.

In the photosensitization experiments, BCA (3 mg/ml) was firstly dissolved in a mixture of ethanol: polyethyleneglycol: water (20:30:50 v/v/v). The resulting solution was diluted in the cell culture medium to achieve the desired concentration of BCA.

2.3. Preparation of liposomes

DMPC (5 mg/ml) was dissolved in chloroform and the solution was dried under vacuum in a rotary evaporator for at least half an hour. Multilamellar vesicles (MLV) were prepared by mechanical stirring (vortex mixer) of the lipid film suspended in PB (pH 7) above the DMPC phase-transition temperature (24°C). Unilamellar liposomes were formed by extrusion of the MLV solution through polycarbonate filters (0.1 μm pore size, Nucleopore Corp., Pleasanton, CA) using a commercial extruder apparatus. This procedure was repeated at least 10 times and led to unilamellar liposomes whose mean size was about 90 nm diameter and whose polydispersity was very low [19]. The stock solution of liposomes was prepared at a lipid concentration of 7.38 mM. BCA in methanol was then incubated with the liposomes at the desired *R* for 30 min in the dark. In our experiments, the final methanol concentration was always lower than 2%.

For the photosensitization experiments, DMPC (15 mg/ml) was dissolved in methanol with cholesterol (0.9 mg/ml) and BCA (0.1 mg/ml). For making the liposomes, the procedure described in the previous paragraph was employed. The mixture obtained was diluted in cell culture medium to achieve the desired concentration of BCA.

2.4. Absorption measurements

The absorption measurements were carried out with a Kontron spectrophotometer (Uvikon 941 instruments) and on a Beckmann DU-64 spectrophotometer. We used quartz cuvettes (Hellma) of 1 cm in both set ups. To reach equilibrium conditions, the solutions were kept 30 min in the dark at each studied temperature before recording the spectra [12]. All the experiments were done at least 5 times.

2.5. Fluorescence measurements

The fluorescence measurements were made on a SLM-Aminco SPF500 spectrofluorimeter (SLM Instruments Inc., USA) with 1 cm Quartz cuvettes (Hellma, Germany). Before recording the spectra, solutions were kept half an hour in the dark at each studied temperature. Corrections for the inner filter effect were performed by using the following formula:

$$F = F_m \times 10^{\frac{(A_{ex} + A_{em})}{2}}$$

where F , F_m , A_{ex} and A_{em} are the real fluorescence, the measured fluorescence, the absorbance at the excitation wavelength and the absorbance at the emission wavelength respectively. All the measurements were repeated at least five times.

2.6. Oxygen consumption

Oxygen consumption of photooxidable compounds was measured with an YSI (Yellow Springs Instruments, USA) model 5300 oxygen consumption meter equipped with a Clarke type electrode. The lamp used was a standard slide projector lamp equipped with a red filter (cut-off wavelength: 590 nm) and the fluence rate above the solutions was 18.4 W/m^2 . The sample cuvettes were immersed in a thermostatic bath. Histidine or ADPA were chosen as substrate.

The Clarke electrode recorded the oxygen level in the solutions during the illumination time. The production of ROS and the subsequent reaction with the substrate leads to a decrease in the oxygen level. The oxygen consumption rate was estimated by calculating the slope of the straight line which fits the beginning of the oxygen level decrease curve. All the measurements were repeated at least three times.

2.7. Electron spin resonance

The ESR measurements were performed in a flat quartz cell at 9.56 GHz on a Bruker ESP 300E spectrometer at room temperature. All the spectra were recorded with a non-saturating microwave power (20 mW) and a modulation amplitude of 1 G. The samples were irradiated directly inside the cavity of the spectrometer using a high pressure xenon vapor lamp (XBO 150 W, Osram GmbH). Light under 600 nm was eliminated by a red cut-off filter (Schott RG610, Germany) set before the cavity of the spectrometer.

2.8. Cell culture

WiDr cells (derived from a primary adenocarcinoma of a rectosigmoid colon carcinoma) were cultured in RPMI 1640 medium containing 10% (v/v) foetal calf serum, 0.1

g/l streptomycin sulphate and 10^5 U/l potassium penicillin, in a humidified atmosphere of 95% air and 5% CO_2 at 37°C .

2.9. Photosensitization experiments

The WiDr cells were seeded in 96-well plates (4×10^4 cells/well) 24 h before the experiments. Cells were incubated for 4 h in the dark with BCA alone (see Section 2.2) or with the BCA-liposomes mixtures (see Section 2.3). The cells were washed with phosphate buffer saline and irradiated in the buffer using a projector lamp followed by a red filter (cut-off wavelength: 590 nm). The fluence rate below the plates was 53 mW/cm^2 . After irradiation, the buffer was replaced by the culture medium, and cells were incubated overnight before each assessment.

2.10. Cell survival

The cell survival was determined by the MTT assay [20]. One hundred (100) μl of MTT solution (5 mg/ml in PBS, diluted 10-fold in serum free medium) was put in each well. Cells were incubated 1 h in the dark at 37°C . The MTT solution was replaced by 2-propanol. After 30 min vortexing the plate on a shaker, the absorbance was read on a microplate reader using a filter of 550 nm. The rate of cell survival was calculated using the following formula:

$$\% \text{ of cell survival} = \frac{Abs_{\text{sample}} - Abs_{\text{background}}}{Abs_{\text{control}} - Abs_{\text{background}}} \times 100$$

where Abs_{sample} , $Abs_{\text{background}}$ and Abs_{control} refer to the absorbance of the sample, the absorbance of the background (well without cells) and the absorbance of the control respectively.

3. Results

3.1. Effect of the temperature on the monomer–dimer equilibrium of BCA and on the oxygen consumption in PB

At room temperature, the BCA absorption spectrum in aqueous solutions at pH 7.0 has its Q_y band between 700 and 850 nm [12], with a main maximum at 757 nm and a secondary one at 792 nm. In PB, BCA is a mixture of monomers and dimers [12]. Due to the great dimerization constant of BCA, it was not possible to obtain by measurements the spectrum of the monomers alone even at concentrations as low as $2 \mu\text{M}$. Nevertheless, using the method of Hoebeke et al. [12], the values of the extinction coefficient at several wavelengths, extrapolated from spectra observed at high concentrations, were slightly lower than in methanol where BCA is only monomeric (data not

shown). Accordingly, like West and Pearce [21], we assumed that the monomer spectrum in PB had the same shape as the spectrum in methanol. Assuming a value of 10^6 M^{-1} (at 25°C) for the dimerization constant and value of $38000 \text{ M}^{-1}\text{cm}^{-1}$ for extinction coefficient of the monomer at 760 nm [12], the dimer spectrum was obtained by subtracting the monomeric part from the total spectrum. Fig. 1(A) shows the Q_y band of the monomeric and the dimeric species of BCA in PB. The Q_y band of the monomer is characterized by a single band with a maximum at 761 nm and the dimer has 2 overlapping bands whose maxima are located at 755 and 792 nm .

The changes of the BCA Q_y band with temperature in PB are shown on Fig. 1(B). The presence of an isosbestic point at 782 nm can be correlated with the co-existence of only two species in the solution: monomers and dimers. When the temperature varies from 14 to 60°C , the second peak (795 nm) decreases and even totally disappears above 60°C which indicates that the concentration of dimers decreases with increasing temperatures. On the contrary, the main peak (760 nm) and the concentration of BCA

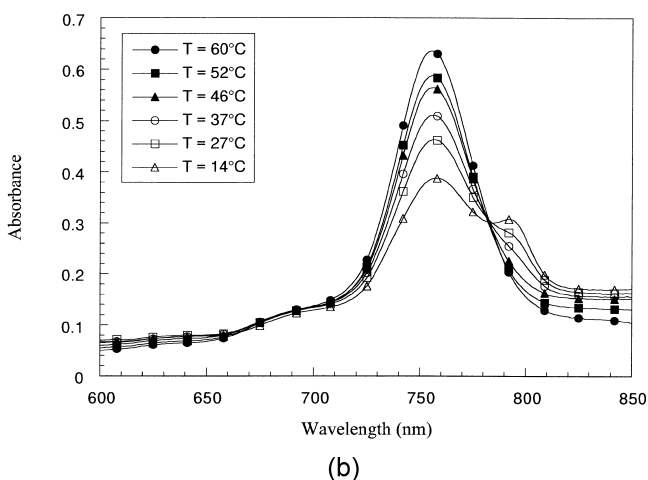
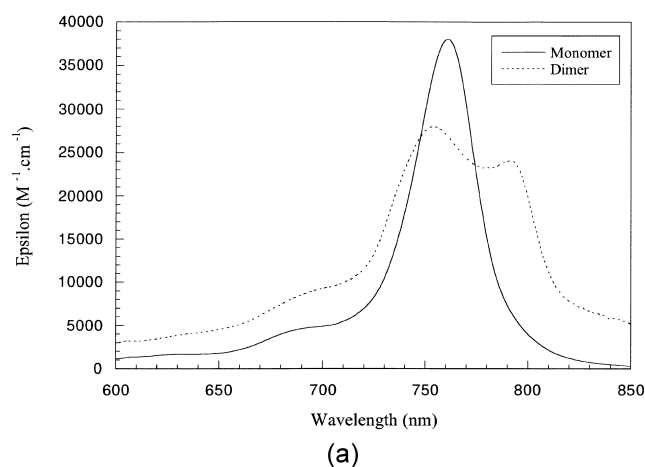


Fig. 1. (A) Simulated absorption spectra of the Q_y band of the monomer and the dimer of BCA in PB. (B) Transformation with temperature of the Q_y band in the absorption spectrum of BCA ($3 \times 10^{-5} \text{ M}$) in PB pH 7.0.

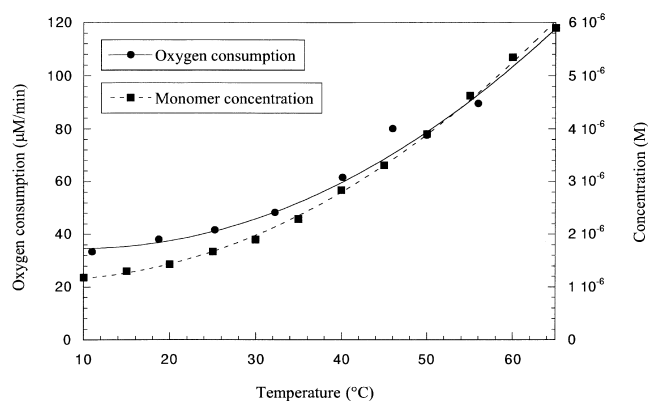


Fig. 2. Increase with the temperature of the concentration of BCA monomer and the oxygen consumption in PB pH 7.0 ($[\text{BCA}] = 2 \times 10^{-5} \text{ M}$). The employed substrate was histidine ($2 \times 10^{-3} \text{ M}$). In the absence of BCA or in the dark, no oxygen consumption was observed (data not shown).

monomers (Fig. 2) increase with increasing temperatures. To calculate the concentration of monomers (C_m), the following procedure was applied (see also [12]). Irrespective of the temperature and the wavelength, the measured absorbance (Abs) for 1 cm optical path is given by

$$Abs = (\epsilon_m \alpha + \frac{1}{2} \epsilon_d (1 - \alpha)) C_t \quad (1)$$

where α is calculated by

$$\alpha = C_m / C_t \quad (2)$$

ϵ_m and ϵ_d are the extinction coefficient of the monomer and the dimer respectively, and C_t is the total concentration of BCA. By combining Eqs. (1) and (2), we obtain C_m :

$$C_m = \frac{Abs - \frac{\epsilon_d}{2} C_t}{\epsilon_m - \frac{\epsilon_d}{2}} \quad (3)$$

At 760 nm , ϵ_m and ϵ_d were equal to $38,000 \text{ M}^{-1} \text{ cm}^{-1}$ and $27,000 \text{ M}^{-1} \text{ cm}^{-1}$ respectively.

Histidine which presents a good reactivity against $^1\text{O}_2$ has been chosen as a substrate for oxygen consumption measurements [7]. The oxygen consumption changes with temperature of an irradiated BCA solution in presence of histidine are presented in Fig. 2. Between 11 and 56°C , the oxygen consumption increases non-linearly with increasing temperature. At 56°C , the oxygen consumption is twice higher than at 11°C . Note that the changes with temperature of the oxygen consumption and the concentration of monomers are similar (Fig. 2). We checked that the effects presented above were not specific to histidine: all the measurements were done at least once with tryptophan or ADPA as substrate. No changes in the shape of the oxygen consumption curves were observed (data not shown).

3.2. Liposomes concentration and temperature effects on the oxygen consumption

In order to check if the incorporation of BCA within liposomes could influence the photodynamic efficiency of BCA, fluorescence and oxygen consumption experiments were carried out. Fig. 3 shows, at 25°C and at pH 7, the oxygen consumption and the fluorescence emission of BCA as a function of R maintaining the BCA concentration constant. The oxygen consumption and the fluorescence curves have the same shape. Both curves increase for increasing R value below 125. For R greater than 125, they remain constant. At these lipid concentrations, the oxygen consumption is nearly 9-fold higher than in PB solutions.

Varying the temperature in solutions with DMPC and BCA could influence the oxygen consumption by modifying the partition of BCA between the lipid bilayer and the aqueous phase. The changes of the BCA incorporation properties in DMPC were followed by fluorescence measurements. Fig. 4 shows the effect of temperature on the fluorescence of BCA in four solutions of different lipid concentrations. The four curves have the same shape: between 10 and 25°C, the fluorescence increases with increasing temperatures, the maximum of fluorescence is reached at 25°C and finally, above this temperature, the fluorescence slowly decreases. The highest concentration of lipids corresponds to a total incorporation of BCA within DMPC at 25°C [14]. Fig. 5 displays the influence of temperature on the oxygen consumption in solutions with BCA completely incorporated into DMPC and BCA in PB (pH 7). In PB, the oxygen consumption slowly increases with increasing temperatures as seen before (see Fig. 2). In liposomes solutions, between 10 and 30°C, the oxygen consumption increases when the temperature is raised and remains almost constant above 30°C.

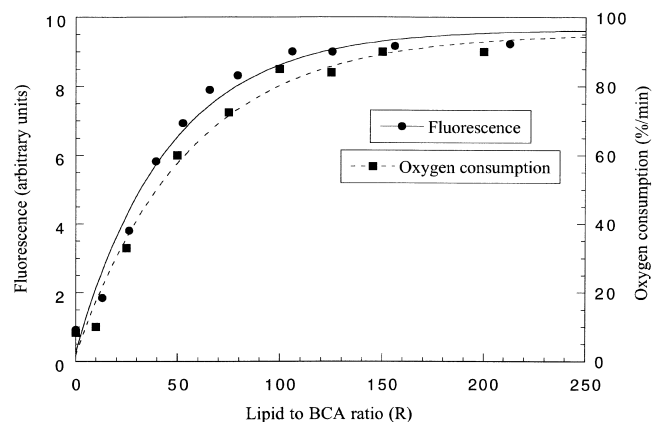


Fig. 3. Influence of the lipids to BCA ratio on the emission fluorescence of BCA (1.2×10^{-5} M) at 775 nm and the oxygen consumption ($[BCA] = 2 \times 10^{-5}$ M). Substrate: histidine (2×10^{-3} M). In absence of BCA in the solutions or in the dark, no oxygen consumption was observed (data not shown). For the fluorescence measurements, BCA was excited at 355 nm.

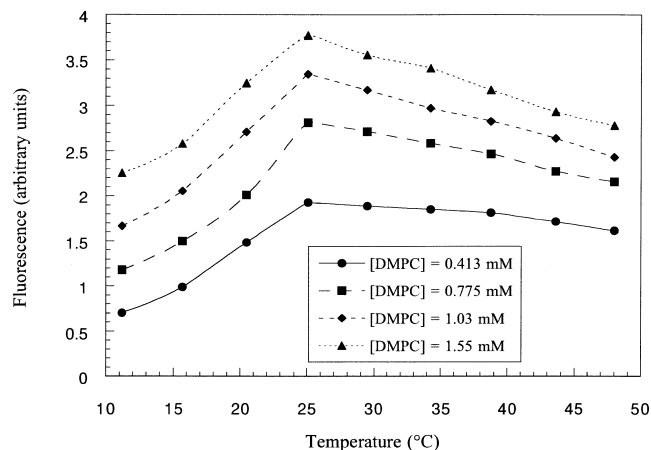


Fig. 4. Influence of the temperature on the BCA incorporation into DMPC liposomes monitored by measuring the emission fluorescence of BCA (1×10^{-5} M) at 775 nm ($\lambda_{\text{excitation}} = 355$ nm). The different DMPC concentrations correspond to R value of 41, 75, 103 and 155.

3.3. Singlet oxygen production in bca-liposomes solutions

To check the involvement of 1O_2 in the oxygen consumption mechanism when BCA is incorporated within DMPC liposomes, competition experiments in the presence of specific quenchers were carried out (Table 1). When ADPA or tryptophan are added to the solution, the oxygen consumption rate increases while it decreases in presence of NaN_3 . Fig. 6 shows the NaN_3 concentration dependence of the oxygen consumption rate in BCA-liposomes solutions. For increasing NaN_3 concentrations lower than 5 mM, the oxygen consumption rate decreases down to 10% of its value without quencher. Increasing the concentration of NaN_3 above 5 mM does not decrease the relative oxygen consumption rate below 10%. Moreover, it was checked by laser flash photolysis experiments that ADPA, histidine, tryptophan and NaN_3 had no interaction with the

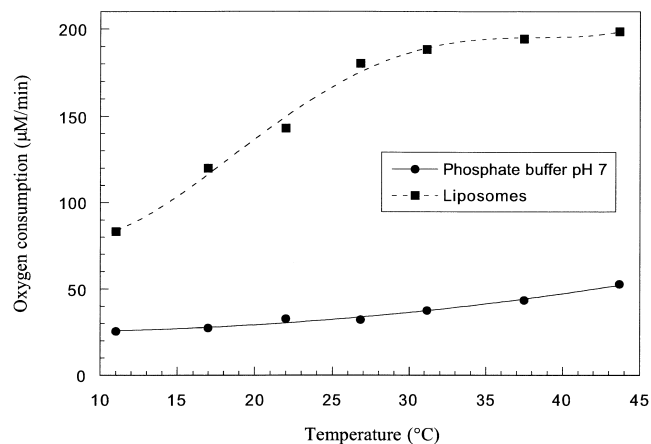


Fig. 5. Comparison of the oxygen consumption in PB pH 7.0 and in liposomes solutions ($[DMPC] = 2.5$ mM) at different temperatures ($[BCA] = 2 \times 10^{-5}$ M). Substrate: histidine (2 mM).

Table 1

Quenchers	Oxygen consumption (nM/min)	Relative oxygen consumption (%)
None	104.45	100
Tryptophan (2×10^{-3} M)	147.27	141
ADPA (2×10^{-4} M)	128.45	123
NaN_3 (2×10^{-3} M)	27.9	26.7

^a Reference: the solution without quencher. Substrate: histidine (2×10^{-3} M).

BCA triplet state under anaerobic conditions. The absence of any effect between BCA triplet state and these $^1\text{O}_2$ scavengers revealed that the effect on the oxygen consumption could only be due to a reaction between $^1\text{O}_2$ and the quenchers.

To detect the presence of $^1\text{O}_2$, we also carried out ESR spin trapping measurements. DMPO, generally used for trapping radicals, was chosen as the $^1\text{O}_2$ spin trap. Feix et al. demonstrated that DMPO is able to react with $^1\text{O}_2$ to produce a [DMPO- $^1\text{O}_2$] complex which decays in the spin-adduct DMPO-OH [24,25]. Fig. 7(A) shows the ESR spectrum produced by the irradiation of a solution containing the spin trap DMPO and BCA incorporated in DMPC. The spectrum obtained is the sum of the DMPO-OH spin-adduct ($a^{\text{N}}=a^{\text{H}}=15$ G) and a second species ($a^{\text{N}}=16$ G, $a^{\text{H}}=22$ G) which could be attributed to the DMPO-MeOH spin-adduct [24,25]. The presence of oxidized DMPO could not be excluded [26]. Adding ADPA (10^{-4} M), a specific $^1\text{O}_2$ quencher, to the solution abolishes nearly all the signal (Fig. 7(B)).

3.4. Cell survival experiments

Our experiments showed that the oxygen consumption rate was higher in solutions where BCA was incorporated in DMPC indicating that BCA could be more efficient in

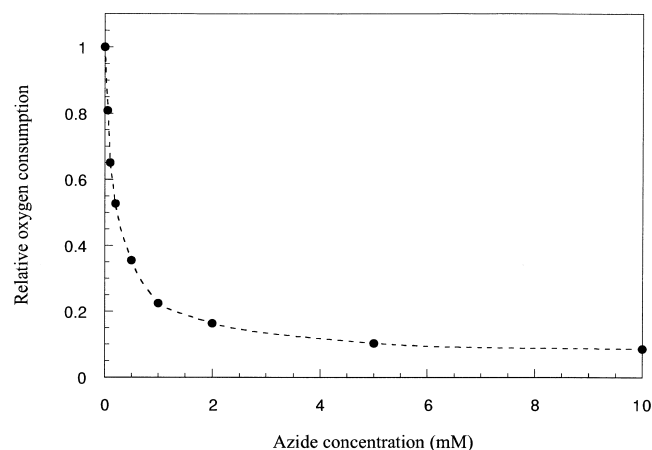


Fig. 6. Decrease of the oxygen consumption in solutions with BCA (10^{-5} M) incorporated in DMPC ([lipids]=1.5 mM) by quenching with azide. All the measurements were carried out at room temperature and pH 7.0. The reference is a solution without quencher. Substrate: ADPA (0.5 mM).

liposomes. The following experiments were carried out to check if using liposomes as drug carriers [13] could enhance the PDT effect of BCA in cells. By the MTT assay, the cell survival of WiDr cells was measured after an illumination with red light for cells incubated with BCA in cell culture medium and cells incubated with BCA incorporated in DMPC (Fig. 8). Irrespective of the BCA concentration, the cell survival is lower when BCA incorporated within DMPC is used. The following control was carried out: the cell survival did not differ significantly from 100% when cells were incubated with DMPC alone (data not shown).

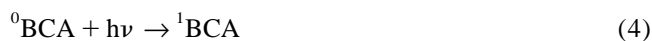
4. Discussion

4.1. Efficiency of BCA in aqueous solutions

PDT is attracting attention because of its potential ability to treat certain cancers and skin diseases [26,27]. The PDT efficacy depends especially on the production of ROS [7–9]. In PB (pH 7), BCA is in a monomer–dimer equilibrium [12] and is able to generate $^1\text{O}_2$ and free radical oxygen species upon illumination [11]. It is worth examining if the temperature, especially by modifying the monomer–dimer equilibrium, has an effect on the production of ROS.

In PB, the temperature induces appreciable transformations in the visible absorption spectrum of BCA which can be attributed to a change in the monomer–dimer equilibrium distribution. Indeed, the increase of the absorbance at 760 nm (peak of the monomer) and the concomitant disappearance of the 795 nm band (one of the two peaks in Q_y band of the dimer) with temperature (Fig. 1) lead us to conclude that increasing temperature favours dye monomerization. This is a common behaviour of aggregated dyes [28,29].

Beems et al. showed that there was an oxygen consumption in aqueous solutions with histidine and BCA irradiated with red light [7]. A mechanism which could explain the oxygen level decrease in solution is described by the following reactions:



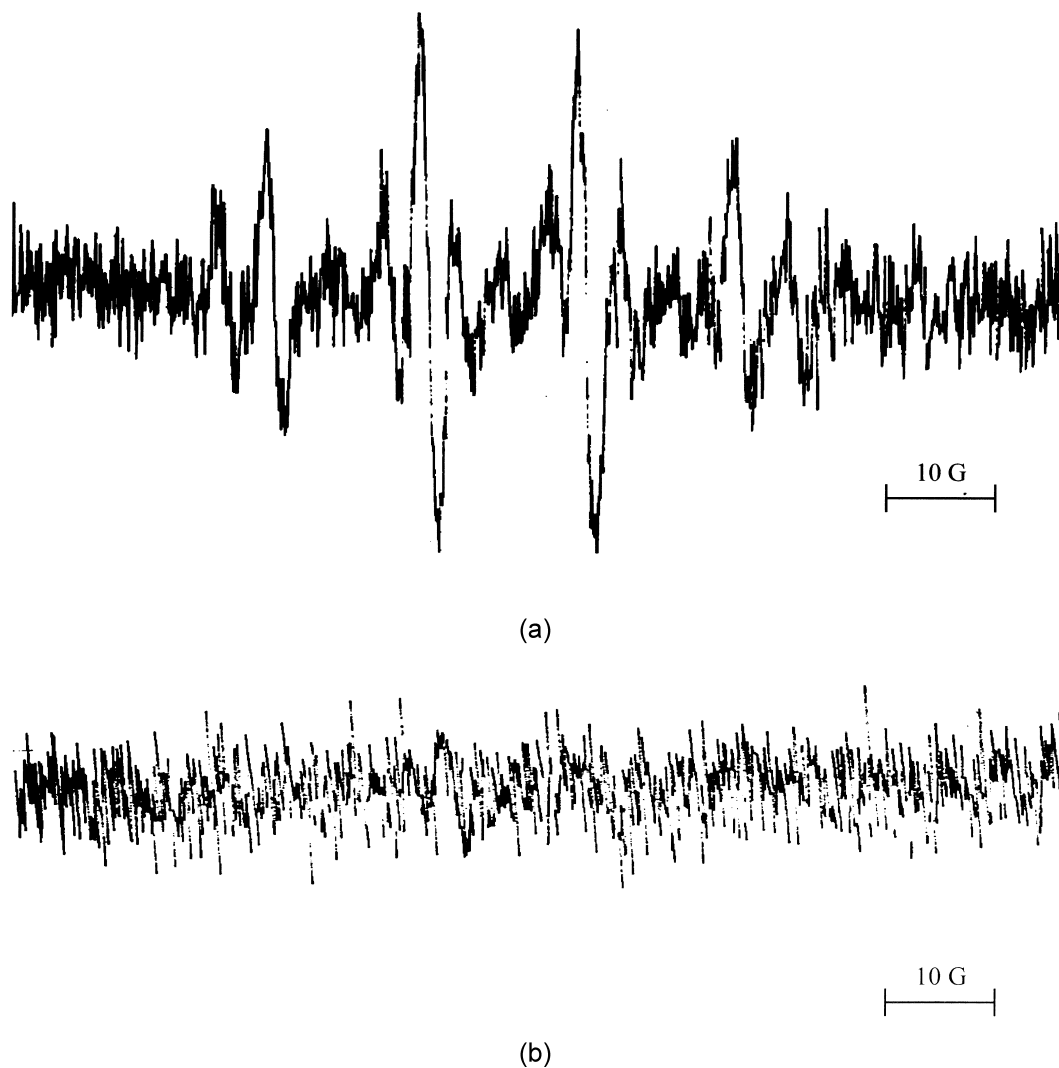


Fig. 7. ESR spectra of spin-trapped ROS obtained by irradiation of BCA (2×10^{-5} M) incorporated in DMPC ([lipids]=3.3 mM) plus DMPO (50 mM) under air: (A) alone (B) in presence of ADPA (10^{-4} M). The concentration of methanol was 2%.

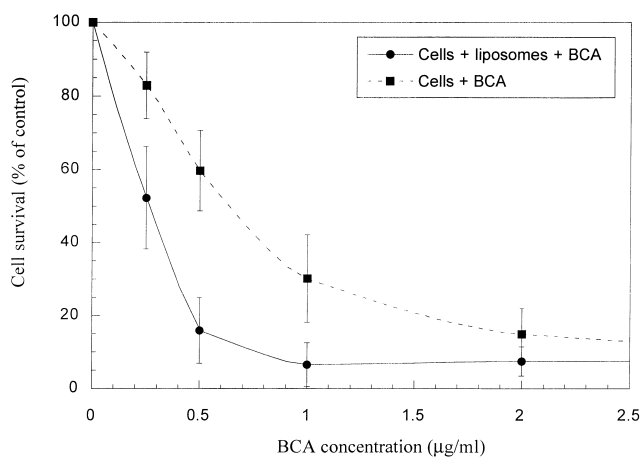


Fig. 8. Effect of the BCA incorporation in DMPC liposomes on the BCA phototoxicity in WiDr cells measured by MTT assay. Cells without BCA and irradiated were used as the control. Cells were irradiated with a fluence of 10 J/cm^2 .



Eqs. (4) and (5) describe respectively the excitation of BCA by light and the decay of the BCA singlet excited state towards its triplet excited state via intersystem crossing. In PB, BCA generates ROS like OH^\cdot and ${}^1\text{O}_2$ by reacting with oxygen (Eq. (6)) [11]. Finally, Eq. (7) shows that oxygen is removed from the solution via a reaction between histidine and ${}^1\text{O}_2$.

As seen in our results, the oxygen consumption rate is influenced by temperature (Fig. 2). The similar temperature evolution of the oxygen consumption and of the concentration of monomers (Fig. 2) allows us to correlate the increase of oxygen consumption to the increase of BCA monomerization. As a consequence, it appears that the monomeric excited form of BCA generates more ROS

than the aggregated one and then has a better photosensitizing efficiency.

4.2. Efficiency of BCA in DMPC liposomes

The aim of our experiments was to check if the incorporation of BCA in a membrane could influence its photodynamic properties and its action mechanisms. DMPC small unilamellar vesicles were chosen because they have saturated lipids and a transition temperature of 24°C easily accessible.

The partition properties between the lipid membrane and the aqueous phase of a dye can be recorded by measuring the emission fluorescence changes of solutions with different lipid concentrations and a constant dye concentration [30]. Hoebeke et al. demonstrated that BCA is partly incorporated in the lipid bilayers if R is below 125 and that it is totally incorporated if R is greater than 125 [12]. They also showed, by absorption experiments, that BCA is only in its monomeric form in the bilayer [12]. So, the increase in fluorescence emission is due to dye monomerization concomitant with dye incorporation within DMPC [29–31]. The similar behaviour of oxygen consumption and the BCA emission fluorescence curves (Fig. 3) shows that the increase in oxygen consumption with increasing R is related to a better incorporation of the BCA in DMPC. Indeed, for $R < 125$, the oxygen consumption increases with increasing degree of incorporation within the liposomes. When BCA is totally within DMPC ($R \geq 125$), the oxygen consumption remains constant at its maximum value. A combination of two factors could explain the increase of oxygen consumption when BCA is incorporated within DMPC. Firstly, using liposomes promotes the monomerization of the BCA [12]. Monomers increase the oxygen consumption since they seem to be more efficient than aggregates (Section 4.1). Secondly the $^1\text{O}_2$ lifetime in the lipid bilayers is longer than in the aqueous phase [32,33]. So, the $^1\text{O}_2$ lifetime in the whole solution is longer than in PB. Consequently, the reaction between $^1\text{O}_2$ and histine (Eq. (7)), which describes the disappearance of oxygen from the solution, is promoted. It should be noted that a reaction between the lipids and ROS is not possible since DMPC are saturated lipids.

It is well known that the maximum incorporation of a dye in liposomes is obtained at the transition temperature of the liposomes [34–36]. Plotting BCA emission fluorescence as a function of temperature shows this well-known effect (Fig. 4). Indeed, below and above the DMPC temperature of transition (24°C), the BCA emission fluorescence, which is related to the incorporation degree of BCA in DMPC, is weaker than at the transition temperature. Our experiments showed that this behaviour was independent of R since the fluorescence curves had the same shape (Fig. 4).

Temperature changes influence the oxygen consumption in BCA-DMPC solutions, especially around 24°C, the

transition temperature of DMPC. The oxygen consumption changes seem to be related to the incorporation of BCA in the bilayers: the oxygen consumption temperature-dependence is nearly similar to the fluorescence one (Figs. 4 and 5). Below 24°C, the oxygen consumption increases with increasing temperature because the incorporation degree of BCA in liposomes increases. However, above 25°C, the oxygen consumption remains almost constant and maximum whereas the fluorescence decreases because of a BCA leakage. It seems that BCA slowly leaks out of the liposomes in the aqueous phase in a monomeric form. Above 25°C, temperature changes do not modify the aggregation state of BCA (monomeric). So, the oxygen consumption remains constant.

4.3. Evidence of the presence of singlet oxygen in DMPC solutions

In PB (pH 7.0), Hoebeke et al. demonstrated by ESR that, under light irradiation, BCA was able to generate $^1\text{O}_2$ and OH^\cdot [11]. In solutions with BCA and DMPC, the oxygen consumption may be the result of ROS production by photoexcited BCA. In order to check the participation of $^1\text{O}_2$ to the mechanism, we used azide, tryptophan and ADPA as $^1\text{O}_2$ quenchers. All the quenchers are water-soluble (they are located only in the aqueous phase) and have an effect on the oxygen consumption (Table 1). These results combined with the fact that the BCA triplet state did not react with the quenchers (see Section 3.3) led us to conclude that $^1\text{O}_2$ was yielded in solution. The differences in the experimental effects observed with the different quenchers are explained by the way the quenchers react with $^1\text{O}_2$. Azide quenches physically $^1\text{O}_2$ producing oxygen in the fundamental state (Eq. (8)) and leading to a decrease of the oxygen consumption. Tryptophan and ADPA react chemically with $^1\text{O}_2$ giving new products by eliminating oxygen from the solution (Eqs. (9) and (10)). Consequently the oxygen consumption increases.



In oxygen consumption experiments with ADPA as substrate, increasing the NaN_3 concentration led to an almost total inhibition of the oxygen consumption (Fig. 6) indicating that $^1\text{O}_2$ could be the main ROS produced. The impossibility to quench completely the oxygen consumption even at high NaN_3 concentration (Fig. 6) could be explained by the localisation of ADPA and NaN_3 . NaN_3 is water soluble and is only located in the aqueous phase. ADPA is partly in the aqueous phase and partly near the water interface of the liposome [14]. Singlet oxygen is generated in the bilayers by BCA. As a consequence, when

$^1\text{O}_2$ diffuse out of the bilayers ADPA has a higher probability than NaN_3 to react with the $^1\text{O}_2$.

To confirm that $^1\text{O}_2$ was produced by BCA in DMPC, we carried out ESR experiments. Our results showed that, upon irradiation, DMPO-OH spin-adducts were generated in solutions where BCA was incorporated in liposomes (Fig. 7(A)). The detection of the DMPO-OH spin-adduct in ESR does not necessarily mean that OH^\cdot were trapped [11,22,23]. Several other sources could induce the appearance of this spin-adduct: (1) a direct interaction between BCA and the spin-trap, (2) the production of $\text{O}_2^{\cdot-}$ followed by trapping $\text{O}_2^{\cdot-}$ by DMPO and decay of DMPO-OOH to DMPO-OH and (3) the production of $^1\text{O}_2$ followed by the formation of a complex between DMPO and $^1\text{O}_2$ and its decay to DMPO-OH and free OH^\cdot (Eqs. (11) and (12)) [11,22,23]. Adding ADPA, a specific $^1\text{O}_2$ quencher, scavenged almost all the DMPO-OH signal (Fig. 7(B)) indicating that $^1\text{O}_2$ was mainly responsible for the DMPO-OH signal formation. It should be noted that direct reactions between DMPO and $\text{O}_2^{\cdot-}$ and/or OH^\cdot coming from the photosensitization of BCA could not be excluded.

The second ESR signal was identified as the DMPO-MeOH spin-adduct. This spin-adduct was probably created by the following mechanism. In a first step, the $^1\text{O}_2$ produced forms a complex with DMPO (Eq. (11)), the complex decays by producing the spin-adduct DMPO-OH and OH^\cdot (Eq. (12)). Due to the high hydrophobic character of BCA, it was impossible to dissolve BCA directly in the aqueous and DMPC solutions. Consequently BCA was firstly dissolved in methanol at high concentration and added in small quantities to the PB or DMPC solutions (see Sections 2.2 and 2.3). In a second step, a reaction occurs between OH^\cdot and the methanol present in solution producing MeOH $^\cdot$ radicals (Eq. (13)). Finally MeOH $^\cdot$ forms with DMPO the spin-adduct DMPO-MeOH (Eq. (14)).



Adding ADPA scavenged also almost all the DMPO-MeOH signal (Fig. 7(B)) confirming the mechanism proposed: the source of OH^\cdot reacting with MeOH (Eq. (13)) is mainly the release of OH^\cdot during the decay of the DMPO- $^1\text{O}_2$ complex (Eq. (12)). A small amount of OH^\cdot from other sources like the photosensitization of BCA could not be excluded.

In PB, BCA is a mixed type I/type II sensitizer [11]. Our results obtained in ESR and oxygen consumption suggested that the incorporation of BCA in liposomes enhanced strongly the $^1\text{O}_2$ production. The production of other ROS species like OH^\cdot and $\text{O}_2^{\cdot-}$ was not excluded.

Nevertheless, the ESR results showed that these mechanisms remain weak. So, BCA within DMPC liposomes acts mainly as a sensitizer of type II.

4.4. Cell survival of WiDr cells

Singlet oxygen is probably involved in the mechanism of PDT which leads to cell death [8,9]. Our results showed that the incorporation of BCA in DMPC increased the $^1\text{O}_2$ production in in vitro experiments. Accordingly, delivering BCA in cells by using liposomes as drug carriers [13] could also increase the photodynamic effect of BCA.

The cell survival experiments carried out on the WiDr cells with BCA showed that, irrespective of the delivery system, BCA was phototoxic for cancerous cells (Fig. 8). Moreover, irrespective of the BCA concentration, delivering BCA by using liposomes instead of BCA in cell culture medium increased the phototoxicity of BCA (Fig. 8) since the cell survival with liposomes is always the lowest. In particular, the cell survival decreased below 15% with BCA-liposomes system, which means that all the cells were killed. It should be noted that with the MTT assay it is not possible to have a cell survival lower than 10–15% even if all the cells are killed [20].

Several factors could explain the decrease of the cell survival when liposomes are used as drug carriers. Firstly, the effect observed could result from different aggregation states of BCA in the cells: BCA could remain in its monomeric form (the species which produce the more $^1\text{O}_2$) in the cells when liposomes are employed while, on the contrary, BCA could be aggregated in cells when it was incubated in cell culture medium. Another factor which may change the PDT efficiency could be the difference of cellular uptake: Schuitmaker et al. showed that the cellular uptake of BCA in presence of cell culture medium decreased by a factor 3 as compared with uptake in PB [16]. So, in our experiments, the BCA uptake may be higher with DMPC. The way BCA is taken up by the cells could also modify its photodynamic cytotoxicity. Schuitmaker et al. showed that, in cell culture medium, BCA is more effective while taken up by the cells via the LDL pathway [16]. Moreover, it has been demonstrated that liposomes enriched with 10% of cholesterol enhance the dye solubilization in LDL [37]. By using DMPC (enriched with 10% of cholesterol, see Section 2.3), we may have favoured the LDL pathway. Finally, the use of the liposomes could also influence the location of the dye in cells. However, it is not actually possible to quantify the importance of each parameters. Further studies are needed to determine the uptake of BCA by the cells, the location of BCA in cells and how BCA are taken up by the cells when liposomes are used as drug carriers.

5. Abbreviations

ADPA 9, 10-Anthracenedipropionic acid

NaN ₃	Azide
BCA	Bacteriochlorin a
DMPC	Dimyristoyl-L- α phosphatidylcholine
MeOH	Methanol
MLV	Multilamellar Vesicle
PB	Phosphate buffer
PDT	Photodynamic therapy
PII	Photofrin II
R	Lipids to BCA ratio
DLL	Low Density Lipoprotein
ROS	Reactive oxygen species
¹ O ₂	Singlet oxygen
OH [•]	Hydroxyl radical
ESR	Electron Spin Resonance
MTT	3-[4,5-dimethylthiazol-2-yl]-2,5-diphenyl-tetrazolium bromide

Acknowledgements

X. Damoiseau thanks the 'Molecular Cell Biology' group of the university of Leiden for their help and kindness during his stays in Leiden. These stays were possible thanks to grants of the French Community of Belgium and the Belgian National Fund for Scientific Research (NFSR).

We would like to thank Marie-Pierre Fontaine-Aupart et Francis Tibel from the 'Laboratoire de Photophysique moléculaire' (University Paris-Sud, Orsay, France) for the laser flash photolysis measurements. We are also indebted to Dr. Jacques Piette for his comments and remarks on this paper.

M. Hoebeke is a Senior Research Associate from Belgian National Fund for Scientific Research (NFSR).

References

- [1] C.J. Gomer, Photodynamic therapy in the treatment of malignancies, *Semin. Hematol.* 26 (1989) 27.
- [2] N. Razum, O.J. Balchum, J.E. Profio, F. Carstens, Skin photosensitivity duration and intensity following intravenous hemetoporphyrin derivatives HpD and DHE, *Photochem. Photobiol.* 46 (5) (1987) 925–928.
- [3] J.J. Schuitmaker, J.A. Van Best, J.L. van Delft, T.M.A.R. Dubbelman, J.A. Oosterhuis, D. De Wolff-Rouendaal, Bacteriochlorin a, a new photosensitizer in Photodynamic Therapy: in vivo results, *Invest. Ophthalmol. Vis. Sci.* 31 (8) (1990) 1444–1450.
- [4] E.M. Beems, T.M.A.R. Dubbelman, J. Lugtenburg, J.A. Van Best, M.F.M.A. Smeets, J. Pierre Boegheim, Photosensitizing properties of bacteriochlorophyllin a and bacteriochlorin a, two derivatives of bacteriochlorophyll a, *Photochem. Photobiol.* 46 (5) (1987) 639–643.
- [5] J.J. Schuitmaker, R.I.J. Feitsma, J.G. Journée-De Korver, T.M.A.R. Dubbelman, E.K.J. Pauwels, Tissue distribution of Bacteriochlorin a labelled with 99 mTc-pertechnetate in hamster Greene melanoma, *Int. J. Radiat. Biol.* 64 (4) (1993) 451–458.
- [6] H.L.L.M. van Leengoed, J.J. Schuitmaker, N. Van der Veen, T.M.A. R Dubbelman, W.M. Star, Fluorescence and photodynamic effects of bacteriochlorin a observed in vivo in 'sandwich' observation chambers, *Br. J. Cancer* 67 (1991) 467–471.
- [7] K. Berg, Mechanisms of cell damage in photodynamic therapy, in: H. Hönlmann, G. Jori, A.R. Young (Eds.), *The Fundamental Bases of Phototherapy*, OEMF, Milano (Italy), 1996.
- [8] B.W. Henderson, A.C. Miller, Effects of scavengers of reactive oxygen and radical species on cell survival following photodynamic treatment in vitro: comparison to irradiation, *Radiat. Res.* 108 (1986) 196–205.
- [9] S. Rywkin, L. Leny, J. Goldstein, N.E. Geacintov, H. Margolis-Nunno, B. Horowitz, Importance of type I and type II mechanisms in the photodynamic inactivation of viruses in blood with aluminium phthalocyanine derivatives, *Photochem. Photobiol.* 56 (4) (1992) 463–469.
- [10] A. Rück, H. Diddens, Uptake and subcellular distribution of photosensitizing drugs in malignant cells, in: H. Hönlmann, G. Jori, A.R. Young (Eds.), *The Fundamental Bases of Phototherapy*, OEMF, Milano (Italy), 1996.
- [11] M. Hoebeke, H.J. Schuitmaker, L.E. Jannink, T.M.A.R. Dubbelman, A. Jakobs, A. Van de Vorst, Electron spin resonance evidence of the generation of superoxide anion, hydroxyl radical and singlet oxygen during the photohemolysis of human erythrocytes with bacteriochlorin a, *Photochem. Photobiol.* 66 (4) (1997) 502–508.
- [12] M. Hoebeke, X. Damoiseau, H.J. Schuitmaker, A. Van de Vorst, Fluorescence, absorption and electron spin resonance study of Bacteriochlorin a incorporation into membrane models, *Biochem. Biophys. Acta* 1420 (1999) 73–85.
- [13] F. Richelli, G. Jori, S. Gobbo, M. Tronckin, Liposomes as models to study the distribution of porphyrins in cell membranes, *Biochem. Biophys. Acta* 1065 (1991) 42–48.
- [14] E. Gandin, Y. Lion, A. Van de Vorst, Quantum yield of singlet oxygen production by xanthene derivatives, *Photochem. Photobiol.* 37 (1983) 271–278.
- [15] M. Hoebeke, E. Gandin, Y. Lion, Photoionisation of tryptophan: an electron spin resonance investigation, *Photochem. Photobiol.* 44 (4) (1986) 543–546.
- [16] J.J. Schuitmaker, J.E. Jannink, T.M.A.R. Dubbelman, Influence of cell culture medium on the photosensitizing effectiveness of bacteriochlorin a, *J. Photochem. Photobiol. B: Biol.* 28 (1995) 143–148.
- [17] T. Omata, N. Murata, Preparation of chlorophyll a, chlorophyll b and bacteriochlorophyll a by column chromatography with DEAE Sepharose CL-6B and Sepharose CL-6B, *Plant Cell Physiol.* 25 (1983) 1093.
- [18] G. Oster, B. Broyde, J.S. Bellin, Spectral properties of chlorophyllin a, *J. Am. Chem. Soc.* 5 (1964) 1309–1313.
- [19] L. Mayer, M. Hope, P. Cullis, Vesicles of variable sizes produced by rapid extrusion procedure, *Biochem. Biophys. Acta* 858 (1986) 161–168.
- [20] T. Mosmann, Rapid colorimetric assay for cellular growth and survival: application to proliferation and cytotoxicity assays, *J. Immunol. Methods* 65 (1983) 55–63.
- [21] W. West, S. Pearce, The dimeric state of cyanine dye, *J. Phys. Chem.* 69 (1965) 1894–1903.
- [22] J.B. Feix, B. Kalyanaraman, Production of singlet oxygen-derived hydroxyl radical adducts during merocyanine-540-mediated photosensitization: analysis by ESR spin trapping and HPLC with electrochemical detection, *Arch. Biochem. Biophys.* 291 (1991) 43–51.
- [23] P. Bilski, K. Reszka, M. Bilski, C.F. Chignell, Oxidation of the spin trap 5,5-dimethyl-1-pyrroline N-oxide by ¹O₂ in aqueous solutions, *J. Am. Chem. Soc.* 118 (1996) 1330–1338.
- [24] E. Finkelstein, G.M. Rosen, E.J. Rauckman, Spin trapping of superoxide and hydroxyl radical: practical aspects, *Arch. Biochem. Biophys.* 200 (1980) 1–16.
- [25] G.R. Buettner, Spin trapping: ESR parameters of spin-adducts, *Free Radic. Biol. Med.* 18 (1987) 1033–1077.
- [26] W.L. Morison, B. Honig, D. Karp, Photochemotherapy for miscella-

- neous diseases, in: H. Hönigsmann, G. Jori, A.R. Young (Eds.), *The Fundamental Bases of Phototherapy*, OEMF, Milano (Italy), 1996.
- [27] C. Abels, A.E. Goetz, A clinical protocol for photodynamic therapy, in: H. Hönigsmann, G. Jori, A.R. Young (Eds.), *The Fundamental Bases of Phototherapy*, OEMF, Milano (Italy), 1996.
- [28] L. Sikurova, R. Frankova, Temperature dependence of merocyanine 540 absorption spectra, *Studia Biophysica* 139 (2) (1990) 103–111.
- [29] C. Balny, S.S. Brody, G. Hui Bon Hoa, Absorption and fluorescence spectra of chlorophyll-a in polar solvents as a function of temperature, *Photochem. Photobiol.* 9 (1969) 445–454.
- [30] D. Brault, C. Vever-Bizet, T. Le Doan, Spectrofluorimetric study of porphyrin incorporation into membranes models-evidence of pH effects, *Biochem. Biophys. Acta* 857 (1986) 238–250.
- [31] D. Brault, Physical chemistry of porphyrins and their interactions with membranes: the importance of pH, *J. Photochem. Photobiol. B: Biol.* 6 (1990) 79–86.
- [32] M. Hoebeke, J. Piette, A. Van de Vorst, Photosensitized production of singlet oxygen by merocyanine 540 bound to liposomes, *J. Photochem. Photobiol. B: Biol.* 9 (1991) 281–294.
- [33] M.A.J. Rodgers, Time resolved studies of 1.27 μm luminescence from singlet oxygen generated in homogeneous and microheterogeneous fluid, *Photochem. Photobiol.* 37 (1) (1983) 99–103.
- [34] M. Langner, S.W. Hui, Merocyanine interaction with phosphatidylcholine bilayers, *Biochim. Biophys. Acta* 1149 (1993) 175–179.
- [35] A. Losi, Fluorescence and time-resolved photoacoustics of hypericin inserted in liposomes: dependence on pigment concentration and bilayer phase, *Photochem. Photobiol.* 65 (5) (1997) 791–801.
- [36] J.R. Lakowicz, *Principles of Fluorescence Spectroscopy*, Plenum Press, New York, 1983.
- [37] J.C. Mazière, P. Molière, R. Santus, The role of the low density lipoprotein receptor pathway in the delivery of lipophilic photosensitizers in the photodynamic therapy of tumours, *J. Photochem. Photobiol. B: Biol.* 8 (1991) 351–360.